Use of rotation numbers to predict the incipient folding of a periodic orbit

S. R. Bishop and C. Franciosi

University College London, Department of Civil Engineering, Gower Street, London WC1E 6BT, UK

(Received January 1986)

This paper predicts the folding of a period orbit. Starting from a general undamped two-dimensional non-autonomous dynamical system a Poincaré section is considered and the resulting two-dimensional discrete system is studied near a fold bifurcation using a new simplified definition of the rotation number. The number's independence from the starting point, as well as its continuity as a function of the control parameters are demonstrated. Scaling properties near the bifurcation are proposed and proved so that predictions of incipient folding instabilities can be made. Finally, the introduction of light damping in the equations of motion is shown not to influence the new definition of the rotation number, so that predictions can still be carried out successfully. The proposed instability prediction method is applied successfully to a digital simulation of Duffing's equation, and to the experimental jump to resonance of an electromagnetically-driven steel beam.

Keywords: rotation numbers, periodic orbit, Poincaré section, Duffing's equation

The main objective of this paper is to predict the incipient folding of a periodic orbit. This research is part of a larger programme exploring possible prediction methods for typical structurally stable modes of instability of equilibria and cycles.

Under one control parameter, equilibrium paths typically lose their stability at either a fold or a Hopf bifurcation.[1] For the fold, a quartic frequency predictor akin to that of the present study has been successfully applied to computer simulations and an experimental column. Studies of the Hopf bifurcation are aimed at predicting the incipient fish-tailing of tankers at single-point moorings.

Steady cycles, and their associated Poincaré maps, typically lose their stability at cyclic folds, flips and Neimark bifurcations. The cyclic folds are discussed in the present paper, albeit under conditions of light damping. The flip bifurcations, which typically trigger sub-harmonic resonances of driven oscillators, are being studied for the bilinear oscillator model of an articulated mooring tower[2] and some encouraging results have been achieved. The Neimark bifurcation has not yet been examined.

Starting from a general two-dimensional non-autonomous undamped dynamical system a Poincaré section is considered and the resulting two-dimensional discrete system is studied near a fold bifurcation, using a new simplified definition of the rotation number.

Hence, the two-dimensional non-autonomous differential system:

$$\dot{x} = F_1(x, y, \mu, t)$$

$$\dot{y} = F_2(x, y, \mu, t) \qquad (1)$$

is considered, in which μ is a control parameter independent of time t, while the functions F_1 and F_2 are assumed to be periodic in time with period T. Due to the periodicity of F_1 and F_2, one can suppose that the variable time is defined on the circle instead of on the whole real axis, so that the states of the system at t and $t + T$ are identified. In this manner, the phase space spanned by x, y and t becomes cylindrical in form, and of interest are the periodic solution curves in this space.

0307-904X/87/02117-09/$03.00

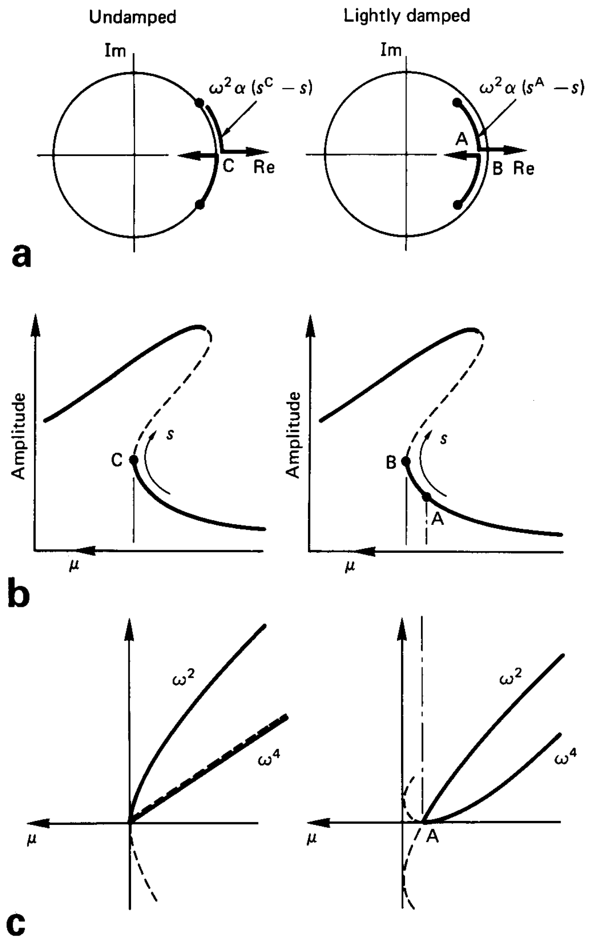

Figure 1 (a) Movement of eigenvalues in complex plane; (b) folding in amplitude response diagram; (c) use of vanishing of mapping or beat frequency to predict incipient folding

A periodic orbit of period kT is defined as a solution curve $X = (x(t), y(t))$ such that:

$$X(t) = X(t + kT)$$

and a fundamental solution when $k = 1$ and sub-harmonic orbit with $k > 1$ can be distinguished.

Defining a two-dimensional Poincaré section in the usual manner, by setting t equal to a constant, it is observed that a sub-harmonic orbit of period kT has its counterpart on the section as k points. The motion of these points on the Poincaré section can be described in principle by a two-dimensional discrete dynamical system, assigning to every starting point on the section its first (directed) return point, which can be written as:

$$x_{i+1} = F(x_i, y_i, \mu)$$

$$y_{i+1} = G(x_i, y_i, \mu) \tag{2}$$

A periodic orbit of period k for the system (equation (2)) is then a set of k points such that:

$$(x_{i+k}, y_{i+k}) \equiv (x_i, y_i)$$

it being presumed that there has been no periodicity of lower order. Hence, if one wishes to study a sub-harmonic orbit of period kT, attention can be focused

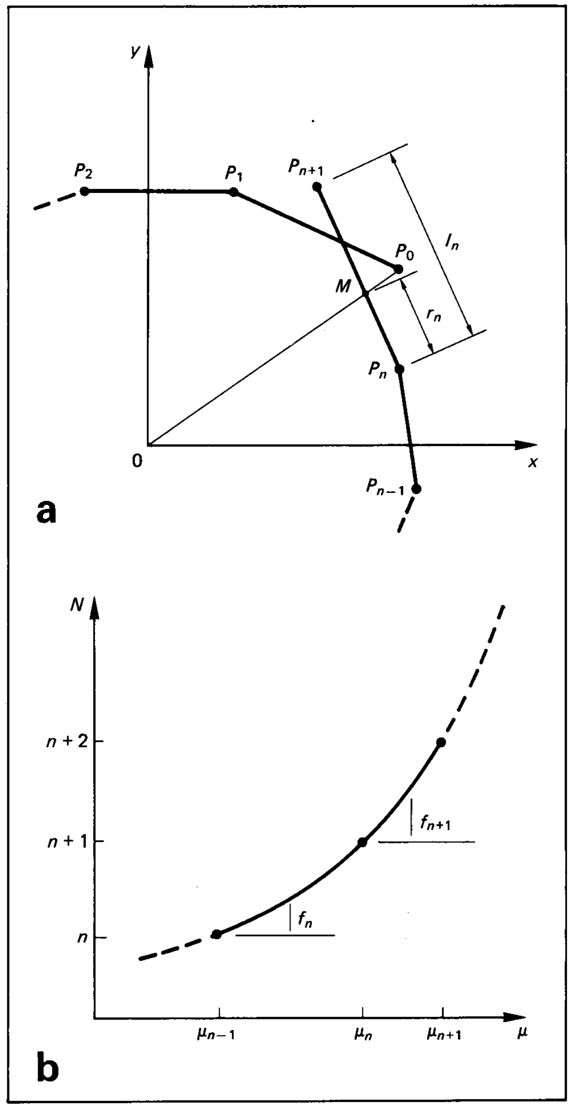

Figure 2 (a) Geometrical definition of orbit number N; $x_{i+1} = ax_i + by_i$; $y_{i+1} = cx_i + dy_i$; $P_i = (x_i, y_i)$; $f_n = r_n/l_n$; $N = n + f_n$. (b) Graph of N plotted against μ to demonstrate continuity of N

on the kth iteration of this Poincaré map that exhibits a fixed point on the corresponding section. This, however, is not written explicitly in the present paper.

Begin by considering an undamped system, for which area is preserved (Liouville's theorem) and the determinant of the Jacobian matrix of the mapping is equal to 1. If the determinant is equal to 1, it is easy to see that both eigenvalues cannot be inside the unit circle, so that the orbit cannot be asymptotically stable. In the same way, it is clear that both eigenvalues cannot lie outside the unit circle. The orbit can thus only be a centre, if the eigenvalues actually lie on the unit circle, or a saddle. These restrictions have some important consequences for the bifurcational behaviour of the system. Suppose in fact that μ is allowed to vary slowly, so that the eigenvalues λ_i of the Jacobian describe paths in the complex plane. The only way in which an eigenvalue can emerge from the unit circle which produces the fold is through the rather pathological route of *Figure 1(a)*,

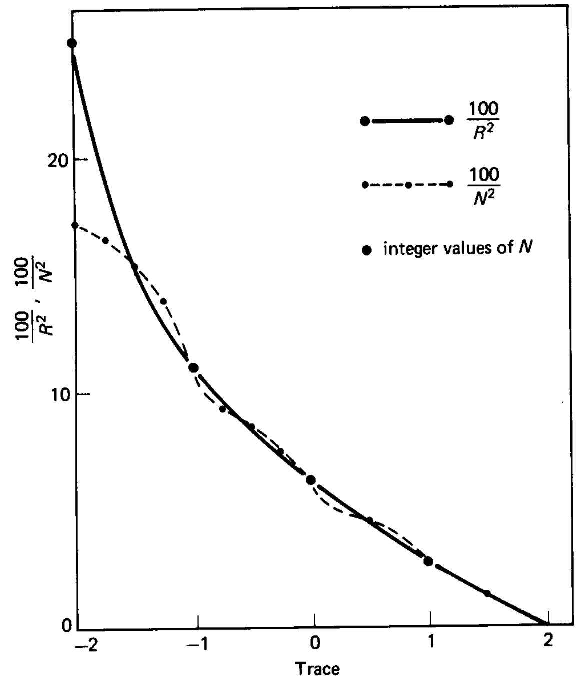

Figure 3 Graphs of $1/R^2$ and $1/N^2$ plotted against trace τ for conservative systems with $D = 1$

in which two eigenvalues become coincident at the bifurcation and then split along the real axis.

This stability transition will normally manifest itself in the response of the parameterized system as a fold in the amplitude response diagram, familiar at the jump to resonance in Duffing's equation as illustrated in *Figure 1(b)*. It is the aim of the present work to identify techniques based on the vanishing of rotation (or beat) frequencies for predicting the approach to such a fold for both undamped and lightly damped systems.

Linearization and definition of rotation number

To examine the stability of the map:

$$x_{i+1} = F(x_i, y_i)$$
$$y_{i+1} = G(x_i, y_i)$$

near a fixed or equilibrium point (x^E, y^E) let:

$$x_i = x^E + \xi_i$$
$$y_i = y^E + \eta_i$$

for all i. Then, considering a Taylor series expansion of the functions $F(x, y)$ and $G(x, y)$ about the fixed point, and using the equilibrium condition gives:

$$\xi_{i+1} = F_x\xi_i + F_y\eta_i + 0(\xi_i^m\eta_i^n)$$
$$\eta_{i+1} = G_x\xi_i + G_y\eta_i + 0(\xi_i^m\eta_i^n)$$

with $m + n > 1$, where the derivatives, F_x, etc. are evaluated at the equilibrium point.

In the neighbourhood of the equilibrium point, for small linear motions, one can neglect the higher order terms to give, in matrix form:

$$\zeta_{i+1} = H\zeta_i$$

where H is the matrix containing the function derivatives and:

$$\zeta_i = \begin{bmatrix} \xi_i \\ \eta_i \end{bmatrix}$$

is a perturbation or error vector.

The necessary and sufficient condition for the convergence of the map to the fixed point is that $\rho(H) < 1$, where $\rho(H)$ is the spectral radius of the matrix H. This may be proved by considering the normal or canonical form of H. However, if the eigenvalues of H are complex conjugate, $\lambda = \alpha \pm i\beta$ say, then it is instructive to note the existence[3] of the matrix Q, such that:

$$H = Q\begin{bmatrix} \alpha & -\beta \\ \beta & \alpha \end{bmatrix}Q^{-1}$$

allowing the change of coordinates:

$$\zeta_i = Q\begin{bmatrix} X_i \\ Y_i \end{bmatrix}$$

Then, making use of the polar representation:

$$X_i = r_i \cos \theta_i$$
$$Y_i = r_i \sin \theta_i$$

it can be shown that:

$$\theta_k = k\theta + \theta_0$$
$$r_k = r_0\rho^k$$

for all integers k, where θ is the argument of the eigenvalues:

$$\theta = \arctan(\beta/\alpha)$$

Then for a map to become unstable, the coefficients, under the influence of the control parameter μ, must vary so that at least one eigenvalue moves outward away from the stability boundary $|\lambda| = 1$.

The well-known instabilities which are the only structurally stable bifurcations under the control of a single parameter (see Guckenheimer and Holmes[4] for a complete study) are the flip and divergence, where a single real eigenvalue crosses the unit circle at -1 and $+1$, respectively, and flutter, where a complex conjugate pair of eigenvalues cross the unit circle and remain complex. Of interest here, however, are undamped two-dimensional maps whose eigenvalues must lie on the unit circle if they are to be stable. The only way in which such a map can become unstable is then via two coincident eigenvalues. Furthermore, attention is focused on the incipient folding to enable consideration of the case when two eigenvalues become coincident at $+1$, as discussed earlier.

Thus, if attention is centred on area preserving maps, then the map is in a condition of neutral stability, and, therefore, local points produced by successive iterations rotate for an infinite number of times neither converging nor diverging. Furthermore, as the coefficients are varied so that the eigenvalues move around the unit circle and approach confluence at $+1$, the number of iterations

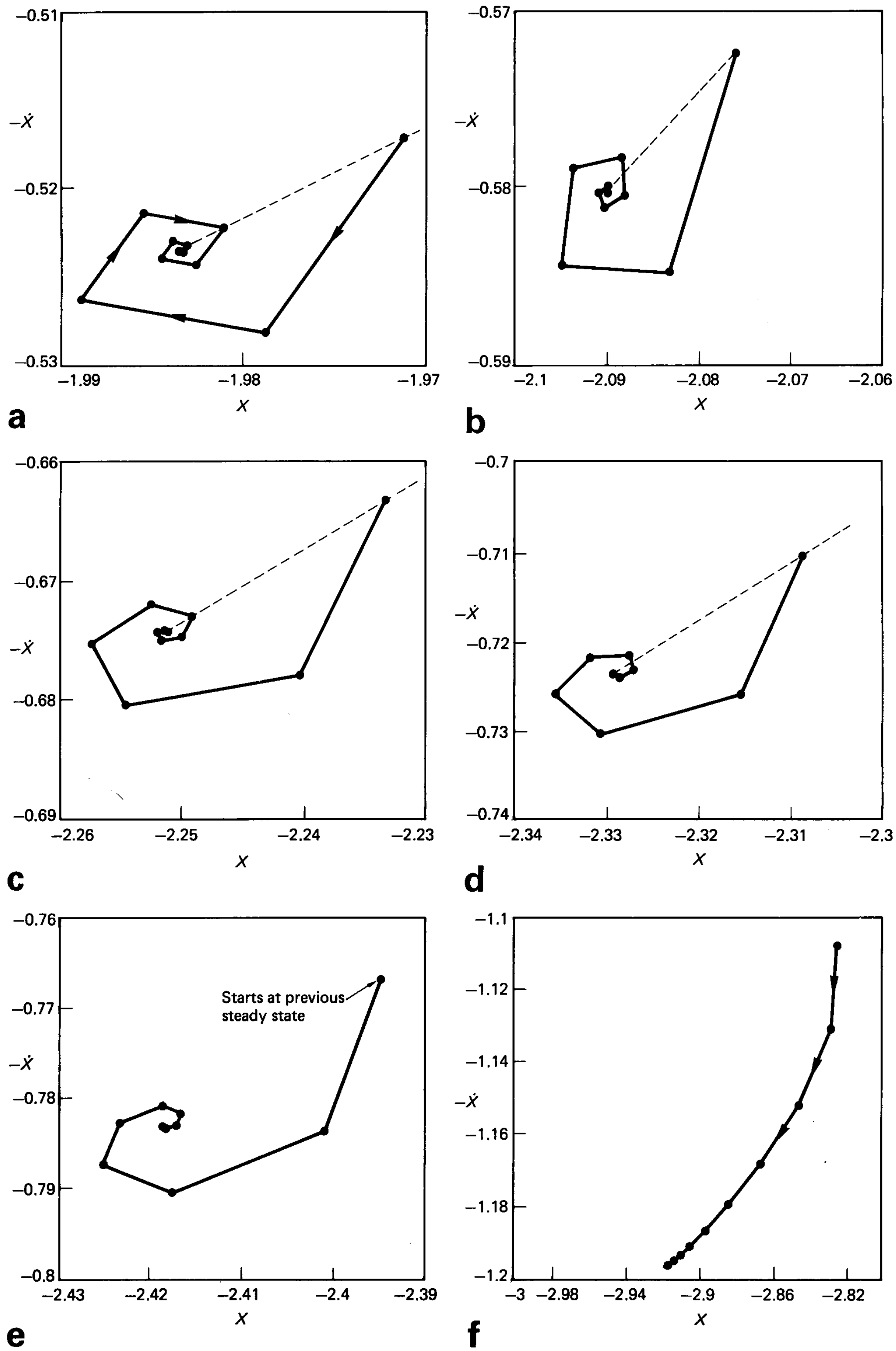

Figure 4 Poincaré maps for Duffing's equation showing increase of rotation number in proximity of fold ($\tau = 2i\pi$): (a) $\eta = 1.530$, $N = 3.99$; (b) $\eta = 1.514$, $N = 4.46$; (c) $\eta = 1.494$, $N = 4.99$; (d) $\eta = 1.486$, $N = 5.49$; (e) $\eta = 1.478$, $N = 5.95$; (f) $\eta = 1.454$, node

of the map required for a complete rotation of 2π about the origin increases.

In order to investigate this behaviour further, the classical definition of rotation number of a map is used as

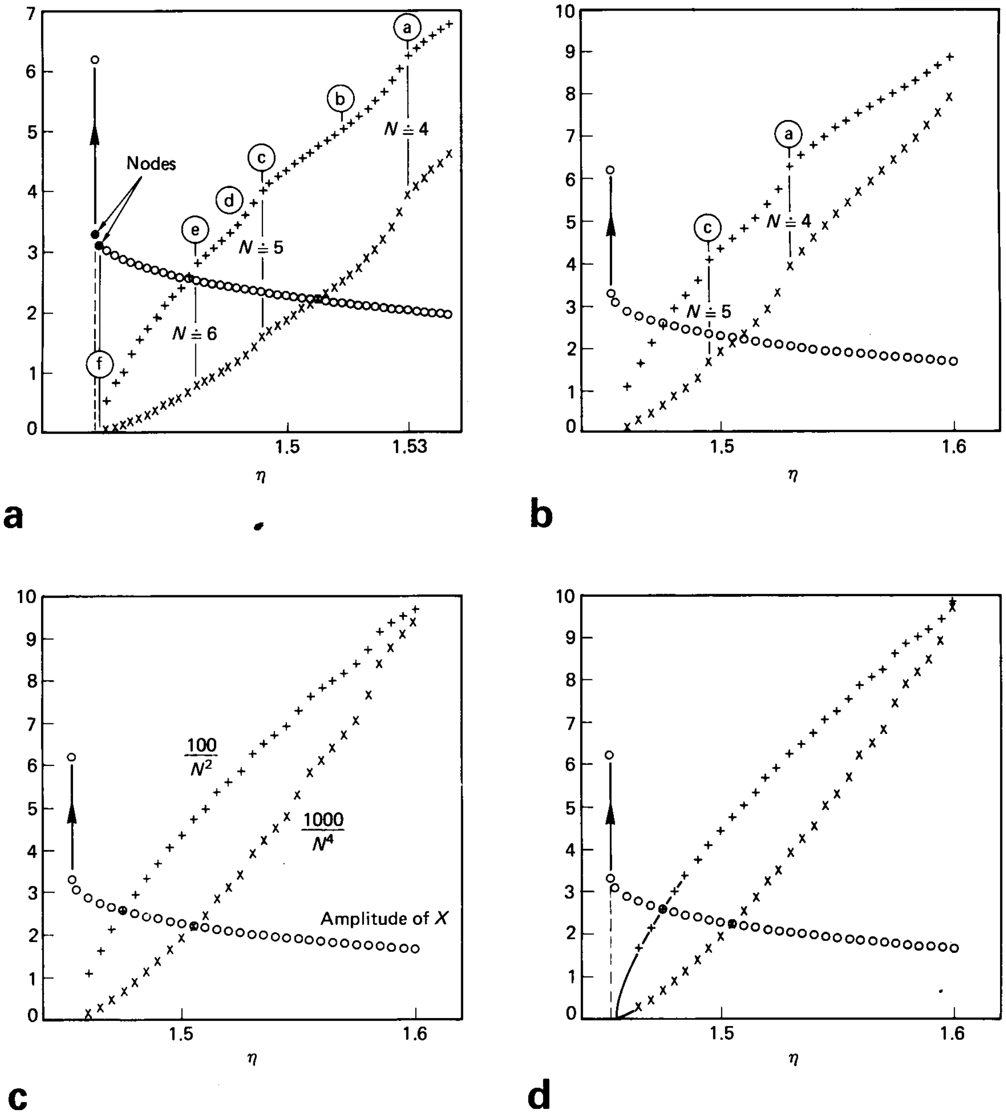

Figure 5 Prediction curves for jump to resonance in Duffing's equation ($\eta^2\ddot{x} + 2\eta\zeta\dot{x} + x + \alpha x^3 = F_0 \cos \tau$, $\zeta = 0.1$; $\alpha = 0.05$, $F_0 = 2.5$): (a) enlargement (one turn); (b) N estimated from one turn; (c) N estimated from three turns; (d) N estimated from five turns

follows. If the $(k-1)$th iteration of the map produces the coordinates (x_k, y_k), which may be represented as (r_k, θ_k) then the rotation number R is given by:[5,6]

$$R = \lim_{k\to\infty} \frac{2\pi k}{(\theta_k - \theta_0)} \tag{3}$$

where θ_k is defined on the real axis and not modulus 2π.

If this limit exists, then the classical definition is valid for a general nonlinear map, but the linear case, may be simplified. As already seen, a similarity transformation may be used to produce a map in the form:

$$x_{i+1} = \alpha x_i - \beta y_i$$

$$y_{i+1} = \beta x_i + \alpha y_i$$

where λ, the eigenvalue of the linear map, is given by:

$$\lambda = \alpha \pm i\beta = e^{\pm i\theta}$$

Then:

$$\theta_k = k\theta + \theta_0 \tag{4}$$

so that:

$$R = (2\pi/\theta)$$

This expression can be simplified still further if $\lambda = e^{\pm 2i\pi\phi}$, with $\phi \in [0, 1)$, so that:

$$R = 1/\phi \tag{5}$$

This definition is a function of the eigenvalues only, and, since eigenvalues are invariant under similarity transformations, this definition may also be used for a general linear map with complex eigenvalues. The frequency of the map rotation is then given by:

$$\omega = 1/R = \phi$$

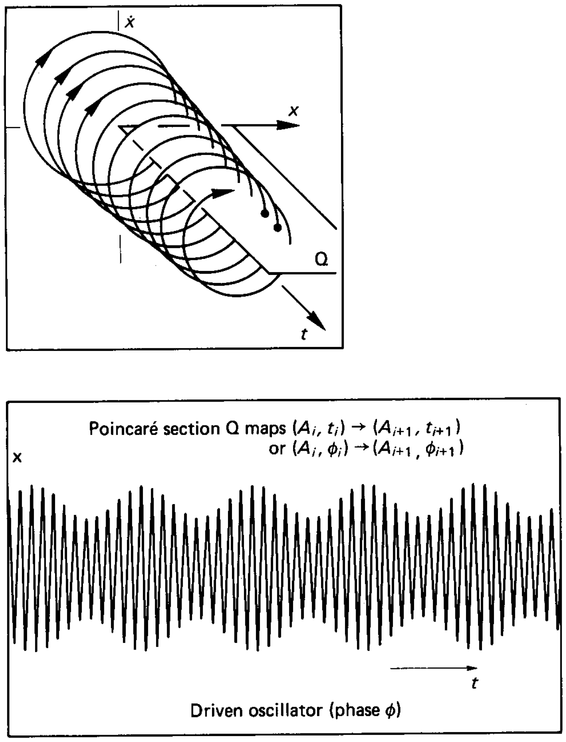

Figure 6 Poincaré section for driven oscillator establishing equivalence of mapping and beat frequencies

It should be noted here that the constancy of angular step implied by equation (4) only holds in this new transformed coordinate, system. It will not, in general, hold in the original space in which the prediction measurements are performed.

Definition of orbit number

As an alternative to the above definition of rotation number, it is possible to use a first approximation to the period. Instead of considering the limiting behaviour, the number n of iterations of the map needed before a single rotation of 2π has been surpassed can be calculated. From a computational point of view, this new approximation has the advantage that it does not require the limit to be evaluated, which is time consuming and, indeed, may also create problems (round-off errors) as the mapping points approach the equilibrium state.

It can be ascertained from *Figure 2* that an orbit number can be obtained by a simple geometrical construction. In fact, it is given by the sum of n, plus the fractional part of the $(n + 1)$th iteration where it intersects the line from the origin to the starting point. This new definition may be written in analytic form as follows. The orbit number N of a two-dimensional map is given by:

$$N = n + f \qquad (6)$$

where n is the least integer such that:

$$|\arg(P_{n+1}) - \arg(P_0)| > 2\pi$$

If the point P_n is given by the coordinates (x_n, y_n), the fractional part f is then:

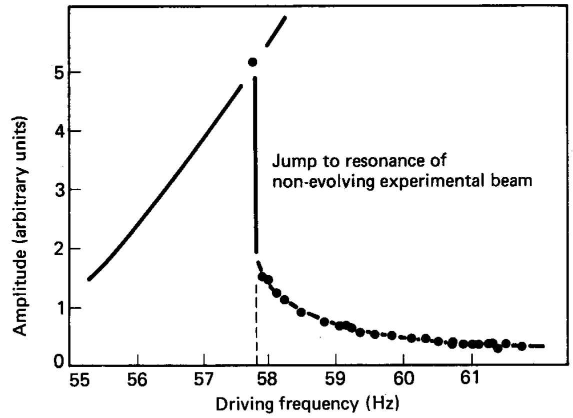

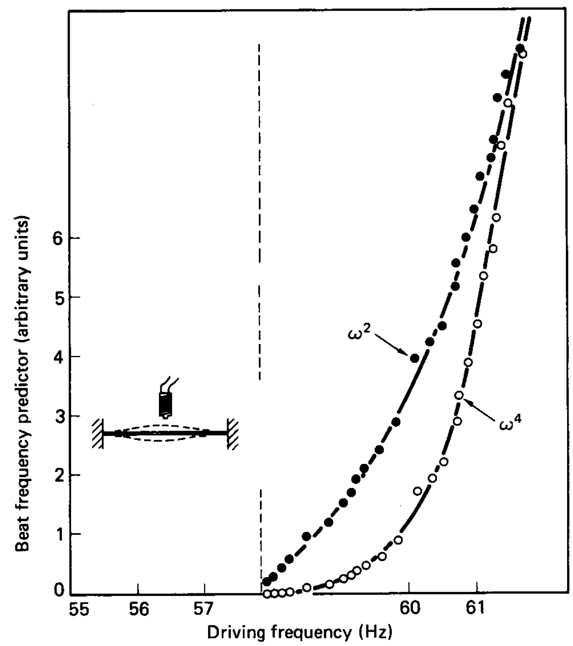

Figure 7 Prediction curves for jump to resonance of experimental beam using square and fourth power of transient beat frequency

$$f = \frac{\overline{P_n M}}{\overline{P_n P_{n+1}}} \left[\frac{(x_m - x_n)^2 + (y_m - y_n)^2}{(x_{n+1} - x_n)^2 + (y_{n+1} - y_n)^2} \right]^{1/2}$$

and the coordinates of $M = (x_m, y_m)$ are found from:

$$y_m = \frac{x_n y_{n+1} - x_{n+1} y_n}{(x_0/y_0)(y_{n+1} - y_n) + (x_n - x_{n+1})}$$

$$x_m = x_0 y_m / y_0$$

To show that this new definition is well posed, it must be proved that it is a function of the trace and a determinant of the linearized matrix, and, hence, independent of starting points.

Theorem

The orbit number of a linear two-dimensional map, area preserving or not, is a function of the trace and the determinant of the coefficient matrix and is independent of initial conditions.

Proof

Consider the general two-dimensional linear map:

$$x_{i+1} = ax_i + by_i$$
$$y_{i+1} = cx_i + dy_i \tag{7}$$

for $i = 0, 1, 2, \ldots$, given $P_0 = (x_0, y_0)$. It is easy to verify that:

$$x_n = R_n(a, b, c, d)x_0 + bS_{n-1}(a, b, c, d)y_0$$
$$y_n = cS_{n-1}(a, b, c, d)x_0 + R_n(d, b, c, a)y_0$$

Letting $Q_n(a, b, c, d) = R_n(d, b, c, a)$ then, for ease of notation, all arguments of the polynomials may be dropped so that:

$$x_n = R_n x_0 + bS_{n-1}y_0$$
$$y_n = cS_{n-1}x_0 + Q_n y_0 \tag{8}$$

provided that the polynomials satisfy the following relationships:

$$R_{n+1} = aR_n + bcS_{n-1}$$
$$S_n = dS_{n-1} + R_n = aS_{n-1} + Q_n$$

For $n > 1$, the polynomial S_n is given by the expression:

$$S_n(a, b, c, d) = \sum_r {}^{n-r}C_r(a + d)^{n-2r}(bc - ad)^r$$

where $r = 0, 1, 2, \ldots, (n - \delta)/2$, $\delta = 0$ if n is even and equal to 1 if n is odd, and where ${}^nC_r$ are the binomial coefficients.

Consequently, S_n may be represented in terms of the trace and the determinant of the coefficient matrix:

$$\tau = a + d$$
$$D = ad - bc$$

as:

$$S_n = S_n(\tau, D)$$

Equations (7) may be used to substitute for x_n, y_n etc. in y_m to yield:

$$y_m = \frac{a_1x_0^2y_0 + a_2x_0y_0^2 + a_3y_0^3}{b_1x_0^2 + b_2x_0y_0 + b_3y_0^2}$$

where the coefficients are given by:

$$a_1 = c(R_nS_n - R_{n+1}S_{n-1})$$
$$a_2 = R_nQ_{n+1} - Q_nR_{n+1}$$
$$a_3 = b(Q_{n+1}S_{n-1} - Q_nS_n)$$

and:

$$b_1 = c(S_n - S_{n-1})$$
$$b_2 = (Q_{n+1} - Q_n) - (R_{n+1} - R_n)$$
$$b_3 = -b(S_n - S_{n-1})$$

This latter equation may now be used in the equation for f to evaluate the fractional part in terms of x_0, y_0 and the polynomials Q_n, S_n, R_n, etc. Finally, by comparing coefficients of x_0 and y_0, and their powers in the numerator and denominator of the resulting expression for f, it is possible, after some algebra, to show that:

$$f = \frac{S_{n-1}}{S_n - S_{n-1}}$$

That is, f depends only upon n and the invariants of the matrix Q.E.D.

It is emphasized that perhaps the more obvious definition of f based on the angular ratio:

$$\frac{|\arg(P_0) - \arg(P_n)|}{|\arg(P_{n+1}) - \arg(P_n)|}$$

would be unsatisfactory since invariance of this definition would be lost.

As previously stated, for the moment the behaviour of an area preserving map is such that the determinant is equal to +1, the eigenvalues of which move round the unit circle. It is useful to put the general matrix in the simplest form that displays these characteristics, namely:

$$x_{i+1} = ax_i - y_i$$
$$y_{i+1} = x_i$$

In fact, any two-dimensional linear map may be transformed into the map:

$$x_{i+1} = b_{11}x_i + b_{12}y_i$$
$$y_{i+1} = x_i$$

via a similarity transformation.

To prove this, consider the two-dimensional linear map of equation (7) in the matrix form:

$$z_{i+1} = Az_i$$

Performing the coordinate change:

$$w_i = Cz_i \qquad C = \begin{bmatrix} c_{11} & c_{12} \\ c_{21} & c_{22} \end{bmatrix}$$

then assuming C^{-1} exists, the map becomes:

$$w_{i+1} = C^{-1}ACw_i$$

and it is clear that:

$$C^{-1}AC = B \qquad B = \begin{bmatrix} b_{11} & b_{12} \\ 1 & 0 \end{bmatrix}$$

is required. Now the trace and the determinant of a matrix are invariant under a similarity transformation as are the eigenvalues, implying that:

$$b_{11} = a + d$$
$$b_{12} = bc - ad$$

Equating the two products AC and CB produces the four equations:

$$-dc_{11} - c_{12} + bc_{21} = 0$$
$$cc_{11} - ac_{21} - c_{22} = 0$$
$$(ad - bc)c_{11} + ac_{12} + bc_{22} = 0$$
$$cc_{12} + (ad - bc)c_{21} + dc_{22} = 0$$

Now, the rank of this linear system is two and so one may choose $c_{12} = c_{21} = 1$, say. Solving the first of these equations yields:

$$c_{11} = (b - 1)/d \qquad d \neq 0$$

from which it may be concluded that:

$c_{22} = cc_{11} - a$

If $d = 0$, then the matrix C is simply given by:

$$C = \begin{bmatrix} 1/c & 0 \\ 0 & 1 \end{bmatrix}$$

Restricting attention to the unit circle, this implies that $b = -1$, with a varying between -2 and $+2$. Under these conditions, the polynomials $S_n(\tau, D) \equiv S_n(\tau)$ are related to the Chebyshev polynomials of the second kind $U_n(z)$

$$S_n(z) = U_n(z/2)$$

The properties of the map along the boundary $D = 1$ are now recovered by the properties of the Chebyshev polynomials, since all the roots of S_n are real and lie in the range $(-2, 2)$. The roots of these polynomials are related to closed orbits as shown in the following section.

Closed orbits

When $\phi = p/q$ say, the system performs exactly p rotations of 2π about the origin in q iterations, so that with $D = 1$ its orbit is formed by q points. The value of the trace corresponding to this value of ϕ is given by:

$$\tau = 2\cos(2\pi p/q) \qquad (9)$$

It is physically evident that the system cannot perform p rotations in q iterations if $p/q > 1/2$. In general, therefore, a system will have $\text{int}(q/2 - 1)$ orbits with q points, where $\text{int}(s)$ is the greatest integer less than or equal to s.

When ϕ is a rational number, the eigenvalues of the system are roots of unit, because if:

$$\lambda, \bar{\lambda} = e^{\pm 2\pi i p/q}$$

then:

$$(\lambda)^q = e^{\pm 2\pi i p} = 1$$

Hence, the closed orbits of the system correspond to eigenvalues that are roots of unity.

On the other hand, a closed orbit of the type $1/p$ must have an orbit number whose fractional part f is 0. This means that $S_{n-1} = 0$ and $S_n = 1$, so that the closed orbits correspond to the second zero of the Chebyshev polynomials. However, all the zeros of these polynomials are given exactly by equation (9) so the rotation and orbit numbers must coincide on the set of integer numbers. More than that, all the closed orbits can be detected using the rotation or orbit numbers.

Comparisons between rotation number and orbit number

A computed graph of $1/R^2$ and $1/N^2$ is shown in *Figure 3* for various values of the trace between -2 and $+2$. From this figure, it can be seen that the two definitions agree very closely in the range $-1 < 7 < 2$. When N is an integer, the two values must coincide. Between two successive values of the trace corresponding to two integer values of N, however, the graph of N exhibits a scallop. This behaviour is clearly evident for small integer values of the period, but if the period is large this behaviour ceases to be apparent, i.e. becomes insignificant.

To explain this in more detail, the continuity of f as a function of the trace must be checked, since N is defined in a piecewise manner. The disconuity, if any, must occur when f changes from 1 to 0. Values of the trace are considered in the neighbourhood of $\tau = \mu_n$, *corresponding to a period of* $N = n + 1$, shown in *Figure 2(b)*. Clearly, the function N is continuous, but it is necessary to check the continuity of its derivative. Defining $N = n + 1 + f_{n+1}$, when τ is in the range $\mu_n < \tau < \mu_{n+1}$, the derivative of f_n and f_{n+1} at $\tau = \mu_n$ can be calculated. For ease of notation, let $\mathrm{D} = \mathrm{d}/\mathrm{d}\mu$ so that:

$$\mathrm{D}f_n = \frac{(S_n - S_{n-1})\mathrm{D}S_{n-1} - S_{n-1}\mathrm{D}(S_n - S_{n-1})}{(S_n - S_{n-1})^2}$$

and:

$$\mathrm{D}f_{n+1} = \frac{(S_{n+1} - S_n)\mathrm{D}S_n - S_n D(S_{n+1} - S_n)}{(S_{n+1} - S_n)^2}$$

Noting from the properties of the Chebyshev polynomials, that:

$$S_{n+1}(\mu_n) = 1$$
$$S_n(\mu_n) = 0$$
$$S_{n-1}(\mu_n) = -1$$

it is easy to show that:

$$[\mathrm{D}f_n]_{\mu=\mu_n} = [\mathrm{D}f_{n+1}]_{\mu=\mu_n}$$

proving that the derivative is also continuous.

It can be shown, however, that the second derivative is not continuous at $\mu = \mu_n$, and it is this discontinuity which causes the scallops. This behaviour becomes more evident in a graph of the square of the required reciprocal of the period.

Instability predictions near a fold

Near a fold, such as that shown in *Figure 1(b)*, the orbit number $N = n + f$ can be approximated by n, so it can be assumed to coincide with the rotation number.

In the neighbourhood of the bifurcation point, the frequency $\omega = 1/N$ drops to zero, and its square ω^2 varies linearly with the trace. In fact, the frequency can be expressed as:

$$\omega = (1/2\pi)\arctan[(4 - 7^2)^{\frac{1}{2}}/\tau]$$

When $7 = 2$ it is possible to expand ω in a power series, obtaining:

$$\omega = \frac{1}{2\pi}\frac{(4 - 7^2)^{1/2}}{\tau} - \frac{1}{6\pi}\frac{(4 - \tau^2)^{3/2}}{\tau^3} + \ldots$$

Hence, the graph of ω^2 against τ is given locally by:

$$\omega^2 = \frac{1}{4\pi^2}\frac{4 - \tau^2}{\tau}$$

and putting $\delta = 2 - \tau$ gives:

$$\omega^2 = (1/4\pi^2)\delta$$

showing that the graph of ω^2 against τ is locally a straight line.

If the system is not area preserving but its determinant is constant and slightly less than 1, the eigenvalues are constrained to move on a path of constant radius as illustrated in the right-hand diagram of *Figure 1*. For such a lightly damped system, the vanishing of ω^2 can be used to predict the value of the trace for which the eigenvalues become coincident.

The definitions of orbit and rotation number, if the latter is defined in terms of the angle ϕ rather than the limit, do not require $D = 1$. Consequently, the vanishing of either R or N can be used to pedict the point of coincidence. If the system is considered to be lightly damped, this coincidence will be close to the fold bifurcation, and thus any instability prediction will be on the safe side.

When considering the general equation (1), at every point on an equilibrium path it is possible to perform a linear stability analysis as previously detailed. Now, considering the trace of the associated matrices it has been shown that ω^2 drops to zero linearly if plotted against some local progress parameter s, say. As can be seen from *Figure 1(b)*, near the fold this parameter varies parabolically with the global control parameter μ. Hence, it is ω^4 and not ω^2 that will drop linearly to zero if plotted against μ. This is strictly true for undamped systems but for lightly damped systems, ω^2 may still be the best predictor.

Applications

(a) Duffing's equation

As an example of the use of the orbit number to predict a fold, consider Duffing's equation in the form:

$$\eta^2\ddot{X} + 2\eta\zeta\dot{X} + X + \alpha X^3 = F_0 \cos \tau$$

This equation involves inertia, linear viscous damping, linear stiffness, a cubic nonlinear stiffness and co-sinusoidal forcing. Choosing η to be the control parameter, and fixing the variables $\zeta = 0.1$, $\alpha = 0.005$ and $F_0 = 2.5$ then the equation exhibits a jump to resonance at a cyclic fold near $\eta = 1.46$. Computed Poincaré maps are shown in *Figure 4* for various values of η in the neighbourhood of the critical point. The orbit number has been calculated for each value of the control parameter using the earlier definition and used to produce the prediction curves shown in *Figure 5*.

The concave nature of the ω^4 prediction curve always allows straight line predictions using the ω^2 curve may appreciably overestimate the critical point unless recordings very close to the fold are taken into account.

The scalloping behaviour of the prediction curves is clearly evident in *Figures 5(a)* and *(b)*. It is possible to reduce the extent of the scallops by calculating the orbit number after more than just a single rotation of 2π about the origin, as shown in *Figures 5(c)* and *(d)*. If the frequency is estimated in this manner, it is clearly closer to the classical limiting definition of rotation number. However, it should be mentioned that in a system with relatively heavy damping, an estimation based on only one 2π rotation might be unavoidable.

(b) Experimental beam

The rotation of a map will manifest itself in an $x(t)$ trace as a low-frequency beat on top of the steady state periodic response. The beat frequency can, therefore, be used in exactly the same way as a map rotation frequency. This is clarified by *Figure 6* which shows that in the three-dimensional phase space of a driven oscillation, the Poincaré section defined by $x = 0$ will present the response amplitude A and the time t as mapping variables, the latter being replaceable by the phase. Thus, the rotation of the amplitude–phase map will manifest itself in the $x(t)$ time history as a beat on the amplitude, as illustrated.

Finally, an experimental study of the frequency predictor is considered using a thin steel beam clamped between two rigig supports and driven to resonance by an electromagnet.[7] The results are summarized in *Figure 7* where the top picture shows the experimentally determined response diagram, with a jump to resonance as the forcing frequency decreases below 58 Hz. The lower diagram shows the two-beat frequency predictors, the beats having been measured manually off an ultraviolet recorder trace. The ω^2 curve is clearly the best predictor, the ω^4 curve approaching the axis with a shallow gradient in an undesirable way. This is clearly because the folding of the amplitude response curve is very local so that its parabolic nature is not significant over the range of forcing frequency considered.

Conclusions

In this paper it has been shown that the rotation number, or alternatively the orbit number, can be used to predict the folding of a periodic oscillation. The two examples discussed here being a numerical solution to Duffing's equation and the jump to resonance of an experimentally driven beam. The method introduced has also been applied to the prediction of the capsize of a rolling ship under the action of regular ocean waves[8]. In this latter example, due to the form of the restoring function, simulations immediately beyond a cyclic fold in the response curve may either restabilize at a large amplitude resonant steady state oscillation or the jump in response may be severe enough so that the vessel capsizes as modelled by a trajectory diverging in infinity. In this particular example the prediction of the coalescence of the eigenvalues just prior to the fold point yields useful information which may be utilized to trigger some form of dynamic positioning of the vessel so as to prevent any imminent disaster. Thus the method forms a useful tool for the prediction of potentially dangerous jumps in amplitude of oscillating systems which can be successfully applied to computer simulations or possibly to guide laboratory experiments.

Acknowledgements

The authors would like to thank Michael Thompson and Lawrence Virgin for many valuable discussions, and also E. T. Sit and M. S. Wu for providing the computational solution of Duffing's equation.

References

1 **Thompson, J.M.T.** Instabilities and catastrophes in science and engineering, *John Wiley, Chichester, 1982*

2 **Thompson, J.M.T., Bokaian, A.R. and Ghaffari, R.** Subharmonic resonances and chaotic motions of a bilinear oscillator, *IMA J. Appl. Math., 1983,* **31,** *207–234*

3 **Hirsch, M. and Smale, S.** Differential equations, dynamical systems, and linear algebra, *Academic Press, New York, 1974*

4 **Guckenheimer, J. and Holmes, P.J.** Nonlinear oscillations, dynamical systems, and bifurcations of vector fields, *Applied Mathematical Sciences, 42, Springer-Verlag, New York, 1983*

5 **Arnold, V.I.** Geometrical methods in the theory of ordinary differential equations, *Springer-Verlag, New York, 1983*

6 **Aronson, D.G., Chory, M.A., Hall, G.R. and McGehee, R.P.** Bifurcations from an invariant circle for two-parameter families of maps of the plane: a computer-assisted study, *Comm. Math. Phys., 1982,* **83,** *303–354*

7 **Thompson, J.M.T. and Virgin, L.N.** Predicting a jump to resonance using transient maps and beats, *Int. J. Nonlinear Mech., 1986,* **21**(3), 205–216

8 **Bishop, S.R., Leung, L.M. and Virgin, L.N.** Predicting incipient jumps to resonance of compliant marine structures in an evolving sea-state, *Proc. 5th Int. ASME Symp. OMAE, Tokyo, April 1986, pp. 179–185. To appear in J.OMAE, Trans. ASME, 1987.*